[1] Zolile Wiseman Dlamini

Data Storage Properties of a Device Based on Selenium-dispersed Cow Milk

Journal of Electrical Systems

Abstract: - The phenomenon of resistive switching in organic materials is crucial for the advancement of devices that have a smaller environmental impact. This work aims to enhance the resistive switching characteristics of organic cow milk-based films by including selenium particles. The non-toxic nature and semiconductor qualities of selenium were the motivating factors behind the decision to utilize it in this work. Four devices were created using milk-selenium active layers with varying selenium concentrations. Upon doing the current-voltage measurements, hysteresis was discovered in all the devices, indicating memory behavior. Our results revealed that higher selenium concentrations led to a decrease in data noise and improved the stability of memory hysteresis throughout repeated measurements. Finally, when the concentration of selenium was too high, the hysteresis became distorted and lost its ability to be reproduced when measurements were repeated. This implies that the resistive switching of cow milk-based devices can be customized by precisely regulating the concentration of selenium particles.

Keywords: Cow milk, selenium, resistive switching memory, hopping conduction.

I. INTRODUCTION

Electrical conduction in biodegradable materials is enthralling, and it appears to be precisely what the world needs to combat the alarming level of environmental pollution caused by electronic waste (e-Waste) [1]. Understanding electrical conduction in biodegradable materials will allow the electronics industry to replace certain device components with biodegradable alternatives or construct entirely biodegradable devices. The industry of computer memory devices is researching alternative data storage technologies. Currently, dynamic random access memory (DRAM) is the predominant "working memory" in computers. This memory has existed for centuries and utilizes a capacitor that, when completely charged, places the device in the ON state, which corresponds to logic "1," and, when depleted, places the device in the OFF state, which corresponds to logic "0." Due to the use of capacitors, DRAMs encounter the following obstacles: (1) As a result of charge leakage in the capacitor, constant data refreshment is required. This refresh consumes a great deal of energy on these devices. (2) The physical size of the capacitor affects the quantity of charge that can be stored, thereby limiting the scalability of DRAMs. The other dominant data storage technology is flash memory. These memories utilize a metal-oxide semiconductor field-effect transistor (MOSFET) with a floating gate. The data is stored by drawing electrons into the floating gate when the device is turned ON and discharging them out when it is turned OFF. Flash memory is a form of high-density nonvolatile data storage that can function as a solid-state drive (SSD) in modern computers [2]. Flash memory's vulnerability is the deterioration of the oxide layer between the normal gate and the floating gate. Therefore, electrons are not completely flushed out of the device, which compromises its functionality.

Resistive switching memories (ReRAMs) are an innovative form of data storage device. In this technology, an active material sandwiched between two electrodes has two distinct and electrically interchangeable resistive states, the high resistive state (HRS) and the low resistive state (LRS). The device is turned ON by changing its resistance from LRS to HRS, and OFF by changing its resistance from HRS to LRS [3; 4]. Tseng et al. also demonstrated that these ReRAM devices can be fabricated using biological materials [5; 6]. Their discovery of resistive switching in tobacco mosaic virus conjugated with platinum nanoparticles paved the way for organic ReRAMs. Aloevera, normal milk [7], chitosan [8; 9; 10; 11], DNA, and a number of other substances have demonstrated resistive switching properties applicable to memory device applications. In addition, a completely flexible and transient ReRAM device made of silk fibroin demonstrates that resistive switching in organic materials has the potential to completely transform the electronic industry [12; 13].

In this investigation, the resistive switching of organic cow milk complexed with selenium (Se) particles is presented. This follows the recent publication of our findings concerning spin-coated ordinary milk on ITO and

[1] Maths, Science and Technology Education, Central University of Technology, 20 President Brand Street, Bloemfontein, Free State, 9300, South Africa

tungsten substrates [7]. In this instance, we chose Se to improve the milk's electrical properties. Se is an earth discovered semiconducting metalloid that is both safe and environmentally beneficial. Selenium is utilized in

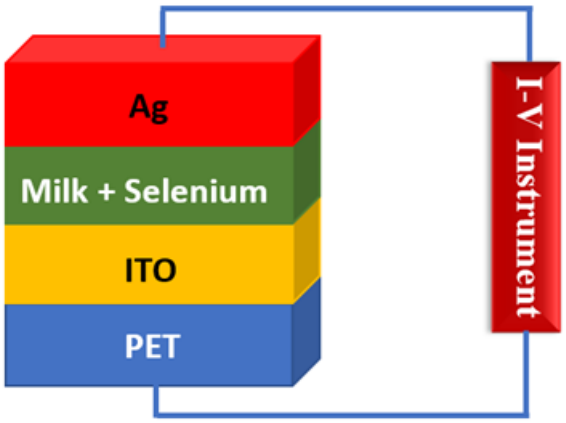

Fig. 1. A schematic diagram depicting the Ag/Milk-Se/ITO-PET device connected to the I-V instrument.

numerous industries, including agriculture [14; 15] and human health supplements [16]. As far as we are aware, Se particles have not been reported to enhance the resistive switching property of a material.

2. Experimental Details

This full cream, homogenized organic cow milk used in this study was acquired from a nearby grocery store. The polyethylene terephthalate coated with indium-doped tin oxide (PET-ITO) substrate, silver (Ag) paste, and selenium (Se) powder were provided by Sigma Aldrich. Before fabrication, the PETITO substrate and beakers were cleansed for contamination with isopropyl alcohol, ethanol, and then distilled water. Our milk-Se films were deposited using the deep-coat process. This process entailed momentarily immersing the PET-ITO substrate in the milk-Se solution, carefully drawing it out, and positioning it with the ITO side facing up so that the film could be formed onto the ITO layer. The substrates were let to dry at room temperature overnight. To make the top electrode, the Ag paste was put on top of the milk-Se film. Fig. 1 displays a scheme of the devices. The following active layers were fabricated in this study: 0.4, 0.8, 1.2, and 1.6 *wt/v*% of Se mass (*g*) into milk volume (*ml*). The following labels are applied to the manufactured devices:

- Ag/milk+Se (0.4)/ITO-PET
- Ag/milk+Se (0.8)/ITO-PET
- Ag/milk+Se (1.2)/ITO-PET
- Ag/milk+Se (1.6)/ITO-PET

3. Resulst And Discussion

3.1. Topography study

The morphology of cow milk, as determined by scanning electron microscopy and X-Ray energy dispersive spectroscopy (EDS), has already been published elsewhere. Fig. 2 depicts the topography investigation of the milk+Se film deposited on the ITO-PET substrate. (a-d). Here, only the composite with the highest (1.6) weight-to-volume ratio is presented. The 10×10 μm^2 3D image depicts a cratered surface with cavities (mapped in green) as deep as 0.36 μm. The roughness in this region is estimated to be 29 *nm*. It is important to note that this image reveals nothing about the Se particles. As a consequence, we conducted a topography study over a 100 by 100 micrometer square area. This region's 3D image (Fig. 2b) clearly depicts Se particles dispersed across the surface, with some plainly visible on the surface. (green and blue mappings). By plotting line profiles from the 2D image (Fig. 2c), we were able to determne the height and diameters of certain protruding particles. The analysis of the line profile (Fig. 2d) reveals particle diameters of 7 μm, indicating that these are Se particles. The thickness of the films used in this study were estimated to be 11.9 μm.

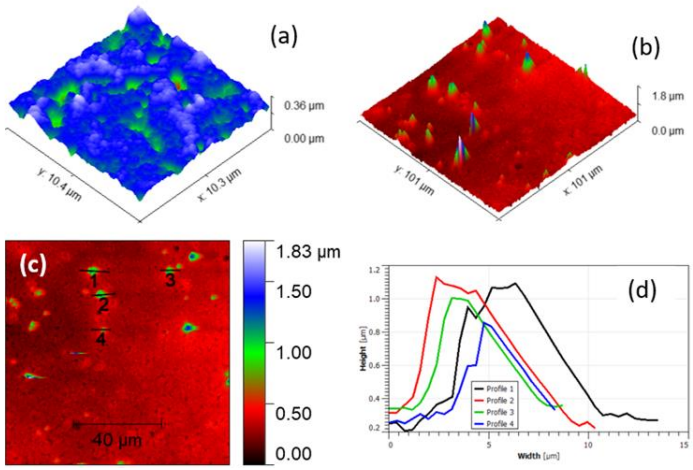

Fig. 2. AFM 3D height trace images taken at 10×10 µm^2 (a) and 100×100 µm^2(b) areas. The replot of the 100×100 µm^2 in 2D(c) showing point selections and their line profile (d).

3.2. Electrical transport and resistive switching study

Using the Keysight source/measure instrument, the electrical characterization of all four devices was carried out. This device permits voltage (V) variations while measuring the current (I) across the device simultaneously. In all measurements, voltage was applied to the top electrode (Ag) while the bottom ITO electrode (BE) was grounded. Throughout the experiments, a voltage variation of 10 *mV* steps with a 25 *ms* delay time and a compliance current (I_{CC}) of 100 μA were maintained as experimental parameters.

The I-V variation of the Ag/milk+As/ITO-PET device is illustrated in Fig. 3 (a-d). To examine the forming phenomenon of the device, a single positive bias voltage scan was performed. The forming process is characterized

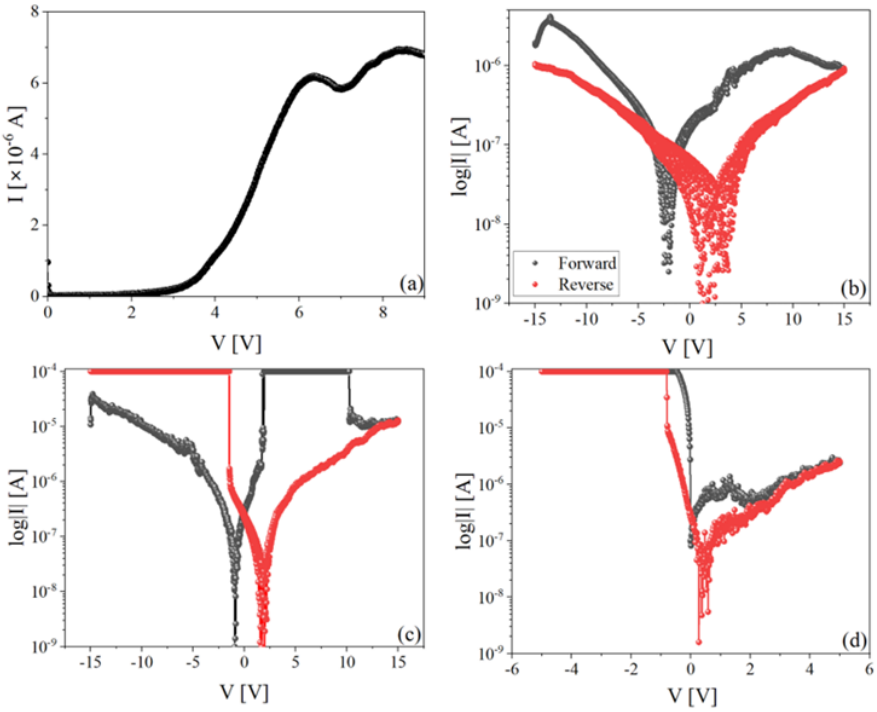

Fig. 3. The I-V characteristics of the The Ag/milk+Se (0.4)/ITO-PET device showing the forming (a), first (b), second (c) and third (d) full cycle voltage scans.

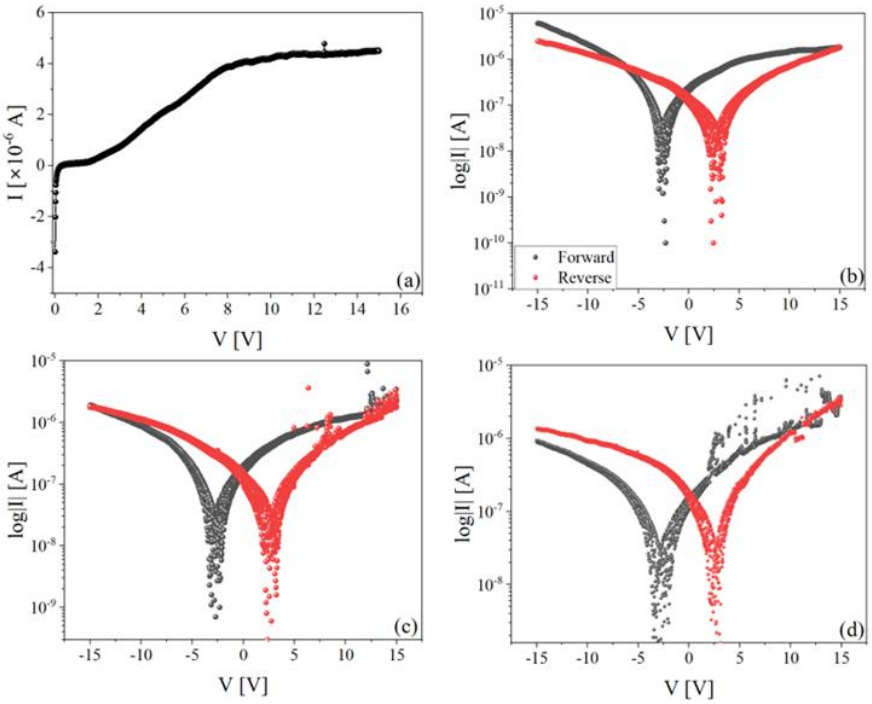

Fig. 4. The I-V characteristics of the The Ag/milk+Se (0.8)/ITO-PET device showing the forming (a), first (b), second (c) and third (d) full cycle voltage scans.

by a sudden jump in current at a particular threshold voltage (V_{form}). In the case of this device, our data do not indicate an abrupt increase in current. Instead, when the voltage is 3 *V* a current is produced, which increases sharply and begins to momentarily decrease at 6 *V*, exhibiting what appears to be negative differential resistance (NDR) behavior [17]. In order to investigate the memory hysteresis, complete cycle voltage scans were performed after examining the forming behavior. The first cycle's results (Fig. 3b) distinct resistive states that indicate memory behavior. In the first cycle, the memory window is −15 to +15 *V*, indicating that this device requires a great deal of power to operate. In addition, the data for the highly resistive state exhibits substantial fluctuations, particularly in the low voltage regime. The second and third cycles depicted in Fig 3 (c) and (d), respectively, exhibit distinct hysteresis and I-V line-shapes, indicating inconsistent device behavior. This device is ineligible for non-volatile memory applications due to its behavior.

The results of the Ag/milk+Se(0.8)/ITO-PET device are illustrated in Fig. 4(a-d). During the initial voltage scan (Fig. 4a), there is no forming occurring. The current remains zero at 0 *V* and begins to increase almost linearly after 2 *V*. The current stopped increasing linearly with voltage after 8 V. The I-V variation graphs for cycles 1 (b), 2 (c), and 3 (d) indicate that the hysteresis stability is enhanced at this Se concentration. However, the low voltage area still has persistent data noise. Furthermore, the negative bias hysteresis also appears to be out of place at these voltages.

In Fig. 5(a-d) the I-V characteristics of the Ag/milk+Se (1.2)/ITO-PET device are illustrated. This device also lacks forming (a). At 0 *V*, the current begins at $+6\times10^{-6}A$ and then decreases swiftly. After that, it follows an ascending trajectory with brief decreases at 1 *V* and 6 *V*. Figures 5 (b) to (f) depict enhanced memory hysteresis classifiable as 'S-type' hysteresis comparable to the keratin device [18]. The line shape is uniform and there is negligible data noise even at low voltage. Furthermore, the memory window for this device is reduced to about −10 to +10 *V* indicating reduction in voltage, thus power needed to run the device. At approximately 5 *V*, the ON/OFF ratio of this device is 10, which makes it possible to discern the ON and OFF memory states. Figure (b) depicts the first cycle, whereas Figures (c), (c) inset, (d), (e), and (f) illustrate the third, fifth, seventh, tenth, and fifteenth cycles, respectively. The fifteenth cycle (f) reveals beginning of data noise at low voltage and a decrease in hysteresis. This device has the potential to be used for non-volatile memory applications with some modifications.

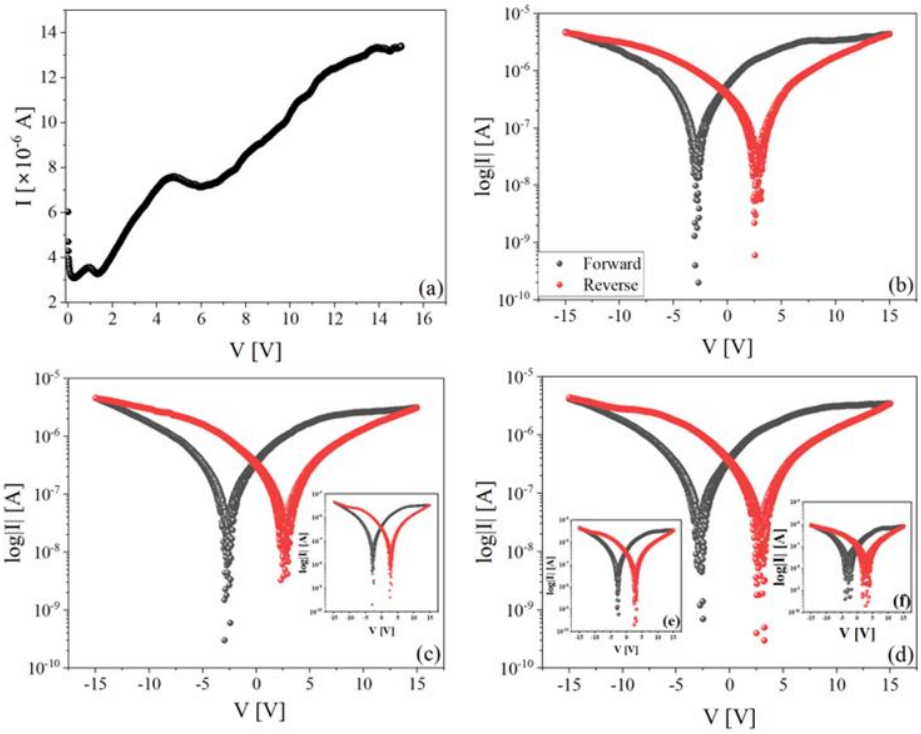

Fig. 5. The I-V characteristics of the The Ag/milk+Se (1.2)/ITO-PET device showing the forming (a), first (b), fourth (c), sixth (c: inset), eighth (d), tenth (e), and fifteenth (f) full cycle voltage scans.

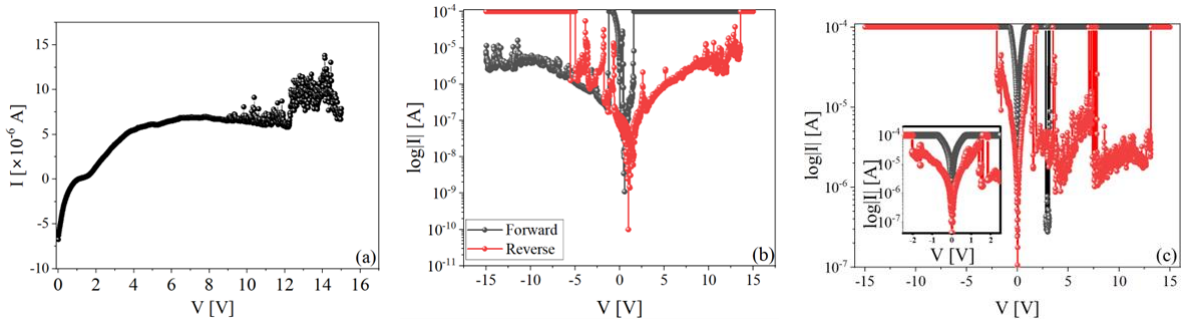

Fig. 6. The I-V characteristics of the Ag/milk+Se (1.6)/ITO-PET device showing the forming (a), first (b), and second (c) full cycle voltage scans.

The I-V characteristics of the Ag/milk-Se(1.6)/ITO-PET device are depicted in Fig 6(a-c). Similarly, this device exhibits no forming. Beginning at $-7\times10^{-6}A$, the current swiftly decreases to zero at 1 *V*. It stays at zero and begins to rise once more at 2 *V*. It begins to decrease at 4 *V* and becomes extremely noisy at 9 *V*. (b) and (c) of Fig. 6 depict full-cycle scans. These graphs have a poor line shape with random spikes in current. This device appears to be predominantly in the LRS, and the desired current level is 100 μA, indicating that the amount of Se in the film exceeds the optimal value needed. Due to the sporadic ups and downs of the current, no application can be derived from the behavior of this device. Among the four devices, the Ag/milk+Se(1.2)/ITO-PET device is deemed to exhibit superior behavior. Therefore, in the following subsection, we will examine its mechanism of conduction.

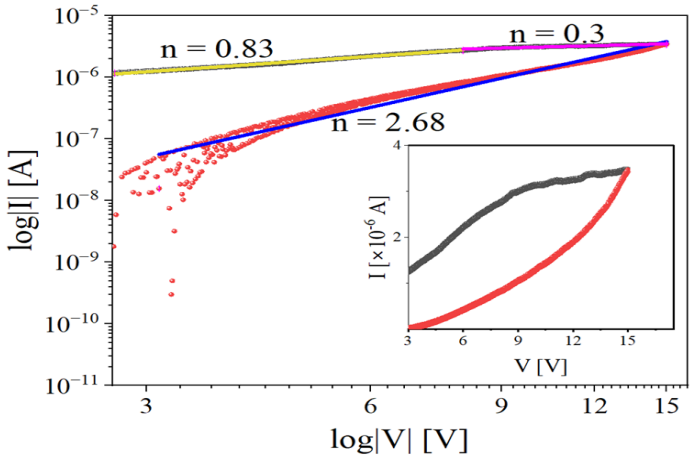

Fig. 7. The log |I| − log |V | and the corresponding I – V graphs the Ag/milk+Se (1.2)/ITO-PET device.

3.3. Electrical conduction mechanism analysis

A viable approach for assessing the conduction mechanism of a ReRAM device involves the graphical representation of the I-V variation data on a logarithmic scale. The slope of the graph can be utilized to approximate the value of n in the $I - V^n$ correlation. The logarithmic plot of the current versus the logarithmic plot of voltage for the positive bias of Fig. 4(d) is presented in Fig. 7. The graph was utilized to perform linear fit analysis, resulting in the determination of slopes of n=2.68 in the HRS, 0.81 in the initial region, and 0.3 in the upper region of the LRS. The value of n =2.68 indicates the phenomenon of hopping conduction in the HRS. The phenomenon of hopping conduction has been detected in systems comprising gelatin and graphene oxide, as reported in the study by [19]. The subsequent is an equation representing the mechanism of hopping conduction.

$$I = I_0 + A\exp\{(V - Va)/kT\} \quad (1)$$

where I_0 represents the residual current, the constant $A(= anv)$, is a product of mean hopping distance, number of electrons and thermal vibrational frequency of electrons at the trap. Va is the characteristic voltage, when multiplied by the electronic charge gives the activation energy. K is the Boltzmann constant [19]. The value of n being approximately equal to 1 in the ON state suggests the possibility of conductive filaments formation within the milk+Se film. These filaments can serve as conductive pathways connecting the top and bottom electrodes. The behavior of the milk-based devices appeared to be highly dependent on the concentration of Se. Therefore, it is feasible that the hopping conduction behavior anticipated by our analysis occurs amidst the Se particles. By dispersing Se with milk, the energy barrier height at the (electrode)/(milk+Se) interface might be reduced, which facilitates the entry of electrons into the milk+As medium. Given the optimal concentration of Se particles, the inter-particle distance (a) is small. Therefore, upon entering the milk+As layer, the electrons undergo a process of hopping between Se particles without experiencing any significant energy loss. As the voltage is increased, the energy barrier height at the interface decreases, which results in an increased influx of electrons into the composite. This may be the reason behind the power function trend observed in our results.

4. Conclusion

The resistive switching characteristic of full cream cow milk has been enhanced through the dispersion of selenium particles. Our research has revealed that an increase in selenium concentration results in a decrease in the hysteresis memory window, an improvement in the ON/OFF ratio, and a reduction in data noise. The optimal results were observed when the concentration of selenium in milk was 1.2 weight per volume percentage. The electron hopping between the selenium particles was identified as the conduction mechanism of this device. This study showcases the feasibility of producing eco-friendly memory devices utilizing organic cow milk. Additionally, the incorporation of semiconductive selenium particles into the milk can enhance the performance of the device.

Acknowledgment

This work was partially supported in part by the CUT & UFS Seed Funding for Multi, Inter - and Trans (MIT) Disciplinary Collaborative Research Grant. Zolile also wants to thank Professor SV Vallabhapurapu for the access to his laboratories.

REFERENCES

[1] P. G. Altbach, W. Li, Q. Liu, Y. Zhang, C. Li, Z. He, W. C. H. Choy, P. J. Low, P. Sonar, and A. K. K. Kyaw, "Biodegradable Materials and Green Processing for Green Electronics," Advanced Materials, vol. 32, p. 2001591, 8 2020.

[2] B. L. Dipert, Inside flash memory, vol. 20. 1995.

[3] Z. Wang, B. Sun, H. Ye, Z. Liu, G. Liao, and T. Shi, "Annealed AlOx film with enhanced performance for bipolar resistive switching memory," Applied Surface Science, vol. 546, no. August 2020, p. 149094, 2021.

[4] B. Sun, S. Ranjan, G. Zhou, T. Guo, Y. Xia, L. Wei, Y. N. Zhou, and Y. A. Wu, "Multistate resistive switching behaviors for neuromorphic computing in memristor," Materials Today Advances, vol. 9, 2021.

[5] R. J. Tseng, C. Tsai, L. Ma, J. Ouyang, C. S. Ozkan, and Y. Yang, "Digital memory device based on tobacco mosaic virus conjugated with nanoparticles," Nature Nanotechnology, vol. 1, pp. 72–77, 10 2006.

[6] Z. W. Dlamini, S. Vallabhapurapu, S. Wu, T. S. Mahule, A. Srivivasan, and V. S. Vallabhapurapu, "Resistive switching memory based on chitosan/polyvinylpyrrolidone blend as active layers," Solid State Communications, vol. 345, p. 114677, 4 2022.

[7] Z. W. Dlamini, S. Vallabhapurapu, T. S. Mahule, and V. S. Vallabhapurapu, "Electrical conduction and resistive switching in cow milk-based devices prepared using the spin-coat method," AIP Adv., vol. 12, no. 9, p. 095321, 2022.

[8] Z. W. Dlamini, S. Vallabhapurapu, O. A. Daramola, P. F. Tseki, R. W. M. Krause, X. Siwe-Noundou, T. S. Mahule, and S. V. Vallabhapurapu, "Resistive Switching in CdTe/CdSe Core–Shell Quantum Dots Embedded Chitosan-Based Memory Devices," Journal of Circuits, Systems and Computers, vol. 31, pp. 1–16, 4 2022.

[9] Z. W. Dlamini, S. Vallabhapurapu, O. A. Daramola, P. F. Tseki, R. W. M. Krause, X. Siwe-Noundou, T. S. Mahule, and S. V. Vallabhapurapu, "Conduction and Resistive Switching in Dropcast CdTe/CdSe Core-Shell Quantum Dots Embedded Chitosan Composite," Iranian Journal of Science and Technology, Transactions A: Science, vol. 46, pp. 709–716, 4 2022.

[10] Z. Dlamini, S. Vallabhapurapu, A. Srinivasan, S. Wu, and V. Vallabhapurapu, "Resistive Switching in Polyvinylpyrrolidone/Molybdenum Disulfide Composite- Based Memory Devices," Acta Physica Polonica A, vol. 141, pp. 439–444, 5 2022.

[11] S. Vallabhapurapu, L. D. V. Sangani, M. G. Krishna, J. Das, A. Srinivasan, and V. V. Srinivasu, "Optical and resistive switching properties of Chitosan-aluminum-doped zinc oxide composite thin films for transparent resistive random access memory application," Journal of Materials Science: Materials in Electronics, vol. 32, pp. 3556–3565, 2 2021.

[12] S.-W. Hwang, J.-K. Song, X. Huang, H. Cheng, S.-K. Kang, B. H. Kim, J.-H. Kim, S. Yu, Y. Huang, and J. A. Rogers, "High-Performance Biodegradable/Transient Electronics on Biodegradable Polymers," Advanced Materials, vol. 26, pp. 3905–3911, 6 2014.

[13] X. Ji, L. Song, S. Zhong, Y. Jiang, K. G. Lim, C. Wang, and R. Zhao, "Biodegradable and Flexible Resistive Memory for Transient Electronics," The Journal of Physical Chemistry C, vol. 122, pp. 16909–16915, 7 2018.

[14] I. Bano, S. Skalickova, H. Sajjad, J. Skladanka, and P. Horky, "Uses of selenium nanoparticles in the plant production," 11 2021.

[15] S. V. Gudkov, G. A. Shafeev, A. P. Glinushkin, A. V. Shkirin, E. V. Barmina, I. I. Rakov, A. V. Simakin, A. V. Kislov, M. E. Astashev, V. A. Vodeneev, and V. P. Kalinitchenko, "Production and use of selenium nanoparticles as fertilizers," ACS Omega, vol. 5, pp. 17767–17774, 7 2020.

[16] M. BODNAR, P. KONIECZKA, and J. NAMIESNIK, "The properties, functions, and use of selenium compounds in living organisms," Journal of Environmental Science and Health, Part C, vol. 30, no. 3, pp. 225–252, 2012. PMID: 22970720.

[17] P. R. Berger and A. Ramesh, "Negative differential resistance devices and circuits," 1 2011.

[18] B. Guo, B. Sun, W. Hou, Y. Chen, S. Zhu, S. Mao, L. Zheng, M. Lei, B. Li, and G. Fu, "A sustainable resistive switching memory device based on organic keratin extracted from hair," RSC Advances, vol. 9, no. 22, pp. 12436–12440, 2019.

[19] S. Vallabhapurapu, A. Rohom, N. B. Chaure, C. Tu, S. Du, V. V. Srinivasu, and A. Srinivasan, "Hopping conductivity-mediated O-shaped memory behaviour in gelatin–graphene oxide composite films," Applied Physics A, vol. 124, pp. 1–5, 9 2018